Both introns and long 3′-UTRs operate as *cis*-acting elements to trigger nonsense-mediated decay in plants

Sándor Kertész[1], Zoltán Kerényi[1], Zsuzsanna Mérai[1,2], Imre Bartos[3], Tamás Pálfy[1], Endre Barta[1] and Dániel Silhavy[1],*

[1]Agricultural Biotechnology Center, Gödöllő, Hungary, [2]Department of Genetics, Eötvös Loránd University, Budapest, Hungary and [3]Institute of Physics, Eötvös Loránd University, Budapest, Hungary

ABSTRACT

Nonsense-mediated mRNA decay (NMD) is a eukaryotic quality control mechanism that identifies and eliminates aberrant mRNAs containing a premature termination codon (PTC). Although, key *trans*-acting NMD factors, UPF1, UPF2 and UPF3 are conserved in yeast and mammals, the *cis*-acting NMD elements are different. In yeast, short specific sequences or long 3′-untranslated regions (3′-UTRs) render an mRNA subject to NMD, while in mammals' 3′-UTR located introns trigger NMD. Plants also possess an NMD system, although little is known about how it functions. We have elaborated an agroinfiltration-based transient NMD assay system and defined the *cis-acting* elements that mediate plant NMD. We show that unusually long 3′-UTRs or the presence of introns in the 3′-UTR can subject mRNAs to NMD. These data suggest that both long 3′-UTR-based and intron-based PTC definition operated in the common ancestors of extant eukaryotes (stem eukaryotes) and support the theory that intron-based NMD facilitated the spreading of introns in stem eukaryotes. We have also identified plant UPF1 and showed that tethering of UPF1 to either the 5′- or 3′-UTR of an mRNA results in reduced transcript accumulation. Thus, plant UPF1 might bind to mRNA in a late, irreversible phase of NMD.

INTRODUCTION

Nonsense-mediated mRNA decay (NMD) is a eukaryotic quality control system that identifies and degrades mRNAs containing premature termination codons (PTC), thereby preventing the accumulation of truncated proteins, which might act as dominant-negative mutants. In addition to eliminating aberrant mRNAs, NMD regulates the expression of wild-type genes, as ~5–10% of the yeast, human or *Drosophila* transcriptome is altered in NMD deficient cells (1–4).

To identify PTC-containing transcripts, the NMD machinery should efficiently discriminate between authentic stop codons and PTCs. At least two (not mutually exclusive) models have been suggested to explain how NMD recognizes PTCs. The first model (often referred to as the pioneer translation or nuclear marking model) suggests that *cis*-acting NMD elements are present in the coding region but not in the 3′-untranslated region (3′-UTR) of wild-type mRNAs. In the nucleus, NMD *trans*-acting factors bind to the NMD *cis* elements and are transported with the mRNAs into the cytoplasm. During the pioneer round of translation, ribosomes displace the NMD *trans*-acting factors from wild-type mRNAs. However, if translation is stopped at a PTC, the NMD *trans*-acting factors bound downstream of the PTC are retained on the mRNA. These mRNA-bound NMD factors recruit further NMD components including UPF1, thereby leading to formation of functional NMD complexes and rapid degradation of the PTC-containing mRNA (5–7). The second model (the *faux* UTR model) proposes that translation termination on PTC-containing mRNAs is aberrant because their 3′-UTR lacks the factors required for normal termination. This model suggests that aberrant translation termination results in assembly of a functional NMD complex, thus leading to rapid decay of PTC-containing mRNAs (8,9).

UPF3, UPF2 and UPF1 proteins are required for NMD in yeast, worm, *Drosophila* and mammals (10). Although these core *trans*-acting NMD factors are conserved, the *cis*-acting NMD elements are different in mammals and in yeast. In mammalian cells, introns are believed to be the predominant *cis*-acting NMD elements (11). When either a U12 or a U2 intron is spliced, a multiprotein complex called the exon junction complex (EJC) is deposited on the mRNA 20–25 nt upstream of each exon–exon junction (12,13). As introns

are rare in the 3′-UTR, the EJC marks the coding regions of mRNAs. UPF3, a component of the mammalian EJC, recruits UPF2 in the perinuclear space. If translation is stopped at a PTC, UPF3–UPF2 complexes located downstream of the PTC can recruit UPF1 and other NMD factors to form functional NMD complex. As translating ribosome remove EJCs located upstream of the stop codon as well as EJCs that are located downstream but in close proximity to a stop codon, mammalian transcripts are targeted by NMD only if a stop codon resides >50–55 nt upstream of an exon–exon junction (14). In yeast, loosely defined sequences called DSE elements can render an mRNA subject to NMD if they are located downstream of a stop codon (15). Hrp1p specifically binds to DSE sequences and might recruit UPF proteins to the mRNAs (16). Both the intron (EJC) and DSE-based PTC definition systems conform to the nuclear marking model. However, a long 3′-UTR can also subject mRNAs to NMD in yeast, *Drosophila* and worm cells (8,17,18). Moreover, mammalian mRNAs with long 3′-UTRs are also targeted by NMD, although less efficiently than mRNAs containing introns in the 3′-UTR (19). The finding that long 5′-UTRs act as NMD *cis* elements can be explained by the *faux* UTR model. Normal translation termination requires the interaction of terminating ribosome and poly(A)-binding protein (PABP). By preventing this interaction, an unusually long 3′-UTR could lead to aberrant termination and formation of functional NMD complex (8,20).

The events of NMD-mediated mRNA decay downstream of functional NMD complex formation are not well understood. In yeast and human cells, NMD complex formation results in decapping and deadenylation of PTC-containing mRNA, while in *Drosophila*, it leads to cleavage of aberrant mRNAs close to the PTC (21). Decapped and/or deadenylated mRNAs are degraded in specific cellular compartments called P-bodies by normal mRNA decay pathways involving XRN1 and the exosome (22). In animals, SMG-1, SMG-5, SMG-6 and SMG-7 are also required for NMD. SMG-1 phoshporylates UPF1, while SMG-5, SMG-6 and SMG-7 are involved in dephosphorylation of UPF1 (23).

NMD also operates in higher plants, although very little is known about mechanism or function of plant NMD systems (24,25). A computer search identified one putative ortholog for UPF1, UPF2 and UPF3 in *Arabidopsis* genome (10). Indeed, alternative splicing products containing PTCs accumulate to high levels in an *Arabidopsis* line carrying a UPF3 mutation (26). Moreover, it has been reported that the null mutant of putative UPF1 is lethal (27,28), while the missense mutant *lba1* shows strong phenotype (27,29). The *cis*-acting NMD elements have not yet been identified in plants. The findings that PTC-containing mRNAs derived from intronless genes are efficiently targeted by plant NMD (30–33) suggest that long 3′-UTRs or DSE-like elements can act as *cis* factors in plants. The role of plant introns in PTC definition is still under debate. In rice waxy gene, splicing of an intron upstream of the PTC affected the efficiency of NMD. These data were interpreted to indicate that splicing and NMD were coupled in plants, as in mammals (34). However, in mammals only introns positioned downstream of the PTC could act as NMD *cis* elements. Moreover, other reports suggested that plant introns present in the 3′-UTR did not subject mRNAs to NMD (35,36).

We have elaborated an agroinfiltration-based transient NMD test system to define the *cis*-acting elements of plant NMD and to identify plant UPF1. We show that both long 3′-UTRs and introns located in the 3′-UTR act as NMD *cis* factors. As both long 3′-UTR-based and intron-based PTC identification systems operate in plants as well as in animals, it is likely that these PTC definition systems already existed in the common ancestor of stem eukaryotes. We have also shown that tethering of UPF1 to either the 5′- or 3′-UTR causes a dramatic reduction of target mRNA levels, suggesting that in plants, UPF1 binds to the mRNA in a late, irreversible phase of NMD.

MATERIALS AND METHODS

Plasmid constructs

For the agroinfiltration assays, genes were cloned into the BIN61S binary vector between the 35S promoter and terminator sequences. Binary vectors contain all *cis* sequences required for *Agrobacterium*-mediated plant transformation or transient expression (37). P14 was previously described (38). Brief descriptions of cloning of unpublished constructs are given here, whereas primer sequences are available as Supplementary Figure 1.

To create binary PHA clone, PHA fragment was PCR amplified with PHA1-F/PHA2-R primers from common bean, cloned first to pBluescript KS, and then it was moved into BIN61S. PCR-based *in vitro* mutagenesis (PHA1mut-F/PHA2mut-R primers) of PHA was carried out with Quik-Change Mutagenesis Kit (Stratagene) to create PHA-m. PHA-s, which contains the ORF of PHA-m from ATG to PTC, was PCR amplified from PHA-m (PHA1-F/PHA2mut-R primers), and then cloned into BIN61S. UPF1 was RT–PCR amplified (Stratagene, ProSTAR®ULTRA HF RT–PCR System) from *Arabidopsis thaliana* leaf RNA with UPF1-F/UPF1-R primers, cloned into pBluescript KS (KSUPF1), and then UPF1 was moved into BIN61S. UPF1DN was obtained by introducing point mutations into KSUPF1 with R863C-F/R863C-R primers, and then the mutant fragment was cloned into BIN61S. To create GFP binary construct, GFP fragment lacking the endoplasmic retention signal was PCR amplified from 35SGFP construct (39) with mGFP4-F/mGFP4-R primers and cloned to BIN61S. *abc, bc, c, b* and *a* fragments were PCR amplified from PHA-m with PHAB1-F/PHAX1-R, PHAB2-F/PHAX1-R, PHAB3-F/PHAX1-R, PHAB2-F/PHAX2-R, PHAB1-F/PHAX3-R primers, respectively. These PCR products were cloned just downstream of the stop codon of binary GFP vector. P-G700, P-G500 and P-G300 PCR fragments were generated with GUS-F/GUS700-R, GUS-F/GUS500-R, GUS-F/GUS 300-R primers, and then these fragments were cloned into PHA-s. ST-LS1 (referred to as Ls in this manuscript) intron was PCR amplified with Ls-F and Ls-R primers from GUS-intron construct (40), it was cloned into pBluescript KS (KSLs), and then it was moved downstream of GFP-*c*. To create P-99Ls, Ls fragment was cloned from KSLs into PHA-s-78 binary vector, which contained PHA-s ORF + 78 nt downstream of PTC. To obtain P-28Ls, PHA-s was cloned to KSLs and then PHA-sLs fragment was moved into BIN61S. To obtain P-28 and P-99 constructs, RT–PCR

products were generated with pFF-R and pKS KpnI primers from RNA samples isolated from P-28Ls and P-99Ls infiltrated leaves, and then these fragments were cloned into BIN61S. λN fragment was PCR amplified with LN-F and LN-R primers from λN construct (41) and cloned into BIN61S. To obtain λN-UPF1, UPF1 from KSUPF1 was cloned into λN binary clone. BoxB tethering target sequence, which contains five direct repeats of boxB, was PCR amplified from 5boxB plasmid (41) with 5BB-F/5BB-R primers, and then it was cloned into the 3′-UTR region of GFP-*c* and PHA-s-78 binary constructs (GFP3′boxB and P-3′boxB). To create GFP5′boxB and P-5′boxB 5′-UTR tethering target plasmids, boxB was cloned into the 5′-UTR region of GFP and PHA-s binary vectors.

Agroinfiltration assays and GFP imaging

Agrobacterium tumefaciens infiltration (agroinfiltration) is a plant transient assay system. Infiltration of *Nicotiana tabacum* or *Nicotiana benthamiana* leaves with culture of an *Agrobacterium* containing a binary vector leads to transient expression of the gene that is cloned into the expression cassette of binary vector. To co-express different genes, agrobacterium cultures each carrying one binary vector should be mixed before infiltration. As agroinfiltration elicits RNA silencing, co-infiltration of a silencing suppressor is required for efficient agroinfiltration-mediated expression. PHA or PHA-derived constructs were agroinfiltrated into *N.tabacum* leaves, while for better GFP visualization GFP and GFP-derived constructs were expressed in *N.benthamiana* leaves. Agroinfiltration assays and GFP detections were carried out as described (42). For co-infiltration, respective *A.tumefaciens* cultures were mixed before infiltration. Unless it is indicated in the text or in the figure legends, the final OD of each culture was 0.2 ($OD_{600} = 0.2$) in the mixture.

Cycloheximide treatment, RT–PCR assay and RNA gel blot analysis

Agroinfiltrated leaves were collected at 3 d.p.i., cut into small pieces and treated for 3 h with 10 μg/ml cycloheximide (Sigma) as described (43). RNA extraction and RNA gel blot analysis was carried out as described (44). PCR fragments labelled with random priming method were used for northern analyses. Phosphorimagine measurements were used to quantify expression of mRNAs. RT–PCR analysis was carried out with QIAGEN OneStep RT–PCR Kit to test splicing efficiency. pFF-R and mGFP4for primers were used for testing the splicing of GFP-*c*Ls. For P-28Ls and P-99Ls samples pFF-R and pKS KpnI primers were used, which amplifies the mRNA of test constructs as well as the mRNA of PHA internal control. PCR fragments were directly sequenced (GFP-*c*Ls) or cloned and sequenced (P-28Ls and P-99Ls).

Western blot analysis

Proteins were separated in an 8% of SDS–polyacrylamide gel, than transferred on to a Hybond-C Extra filter (Amersham Pharmacia Biotech). N-terminal region of UPF1 (1–123 amino acids) was expressed as a glutathione *S*-transferase (GST) fusion protein in *Escherichia coli* (GST-UPF1-N), then rabbit polyclonal antibodies (α-UPF1) raised against GST-UPF1-N were used for western analysis.

Transiently expressed *Arabidopsis* UPF1 or UPF1DN proteins were easily detected with α-UPF1, while endogenous *N.tabacum* or *N.bethamiana* UPF1 could not be detected with this antibody.

RESULTS

Agroinfiltration-based transient NMD test system

Transient assays have been successfully used to study NMD in mammals and *Drosophila*. Therefore, as a first step towards characterization of plant NMD, we wanted to establish an efficient transient NMD assay system. It has been shown that the wild-type bean phytohemagglutinin (PHA) mRNA is stable, while the mutant mRNA containing a PTC (PHA-m) is efficiently targeted by NMD (30,31). In transgenic tobacco cells, the half-lives of PHA-m transcripts were reduced 3-fold relative to the PHA transcripts; consequently PHA-m mRNAs accumulated to ∼5 times lower levels than PHA transcripts (31). We have adapted this well-characterized NMD reporter gene system to establish an agroinfiltration-based transient plant NMD assay (also see Materials and Methods). PHA and PHA-m, which contains a PTC at codon 79, were cloned into binary vectors (Figure 1), and then *N.tabacum* leaves were infiltrated with *Agrobacterium* cultures carrying PHA or PHA-m binary plasmid. As an internal control, the ORF of PHA-m from ATG to the PTC (PHA-s) was also cloned into a binary vector (Figure 1), and then the *Agrobacteriu*m-containing PHA-s was co-infiltrated with either PHA or PHA-m. Moreover, as agroinfiltration leads to strong transgene-induced RNA silencing, P14 silencing suppressor (Figure 1) was also co-infiltrated (38). Thus, leaves were co-infiltrated with PHA + PHA-s + P14 or with PHA-m + PHA-s + P14 cultures. At 3 days post infiltration (d.p.i.) RNA gel blot assays were performed to monitor mRNA accumulation. PHA and PHA-m transcript levels were normalized to the levels of the PHA-s common internal control; therefore PHA and PHA-m mRNA levels could be compared. The finding that PHA-m mRNA levels were ∼10 times lower than PHA mRNA levels suggested that PHA-m transcripts were targeted by NMD (Figure 2A, compare lanes 3–4 to 1–2 and Supplementary Figure 2). As NMD is a translation-dependent RNA degradation system, treatment with the translation inhibitor cycloheximide stabilizes PTC-containing mRNAs. To confirm that NMD is responsible for the reduced PHA-m mRNAs levels, PHA and PHA-m infiltrated leaves were treated with cycloheximide. As expected, cycloheximide treatment resulted in strongly increased PHA-m mRNA levels (3.75×), but did not enhance PHA mRNA accumulation (Figure 2B). These data support the conclusion that in agroinfiltrated leaves PHA-m mRNA levels are downregulated by NMD.

In worms, the NMD and RNA silencing pathways overlap (45). Thus, because UPF1 may be involved in RNA silencing in plants (28), it was possible that the P14 silencing suppressor modified the NMD response. To exclude this possibility, we repeated the experiments in the absence of P14 but at a lower temperature (15°C), where RNA silencing is inactive (46). We found that at 15°C, in the absence of P14, PHA-m mRNAs accumulated to much lower levels
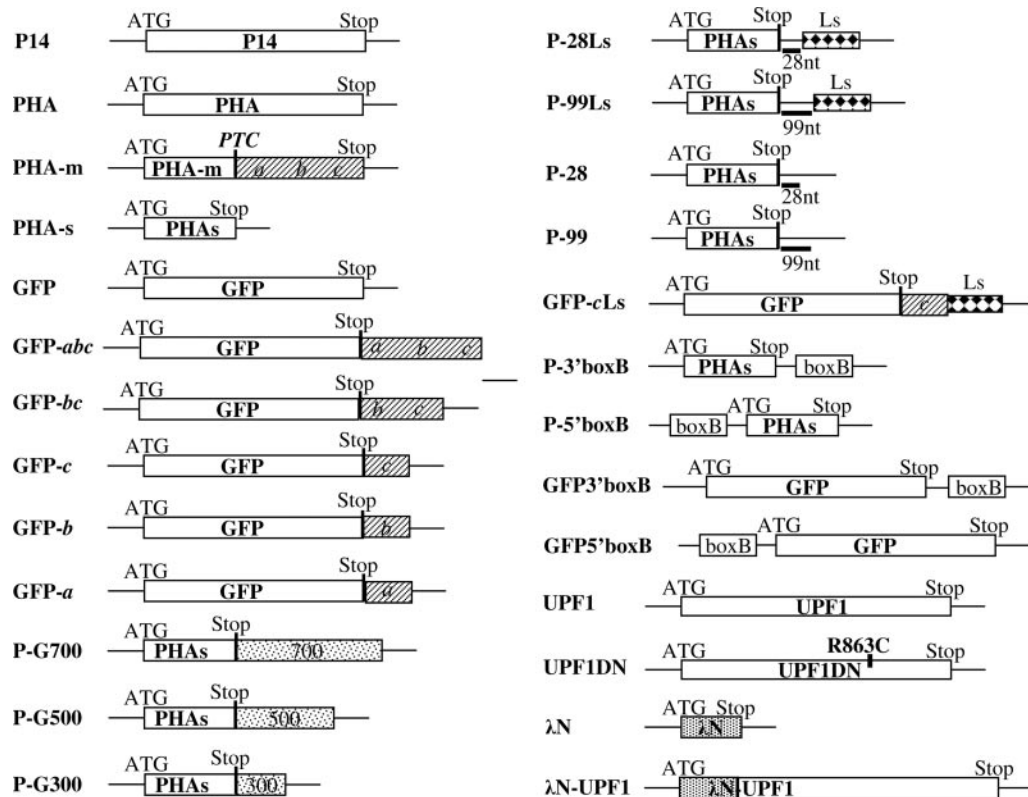
Figure 1. Schematic representation of binary constructs used in this work.

than PHA transcripts (Figure 2C). These data suggest that, in contrast to RNA silencing, NMD is active even at low temperature and indicate that P14 does not affect NMD. Consistently, PHA transcripts were ∼10 times more abundant than PHA-m mRNAs when these genes were expressed at the normal growth temperature from a specific binary vector (NOSas) that barely triggers silencing (S. Kertesz, Z. Merai and D. Silhavy, unpublished data).

As these data suggest that P14 has no effect on NMD, further agroinfiltration-based NMD experiments were carried out at 22°C in the presence of the P14 silencing suppressor.

Identification of *Arabidopsis* UPF1

UPF1 is the key *trans*-acting factor responsible for NMD in yeast as well as in animals. Based on sequence similarities, it has been suggested that At5g47010 encodes UPF1 (UPF1) in *Arabidopsis* (10,27). Moreover, as many PTC-containing transcripts are upregulated in a missense mutant or in T-DNA insertion mutants of At5g47010, it is likely that *Arabidopsis* UPF1 is a functional ortholog of yeast UPF1 (28,29). However, direct evidence proving that *Arabidopsis* UPF1 is involved in NMD have not yet been reported. To test whether plant UPF1 plays a role in NMD, it was amplified by RT–PCR, cloned into a binary vector, and then the effect of overexpression of UPF1 on NMD was studied in agroinfiltration assays. As co-infiltration of UPF1 did not result in increased PHA-m transcript levels, we concluded that overexpression of *Arabidopsis* UPF1 did not affect NMD in tobacco leaves (data not shown).

It has also been reported that changing of a conserved arginine to cysteine in the RNA helicase domain of either yeast (R779C) or human (R844C) UPF1 leads to a dominant-negative protein (47,48). We hypothesized that if At5g47010 encodes the functional *Arabidopsis* UPF1, a similar change of the corresponding arginine (R863C) will also lead to a dominant-negative protein (UPF1DN, see Figure 1), and that expression of UPF1DN will interfere with NMD. To test these hypotheses, PHA-s control and PHA-m NMD reporter constructs were co-infiltrated with UPF1DN. Importantly, co-expression of UPF1DN selectively increased the levels of PTC-containing PHA-m transcripts, providing evidence that UPF1DN interfered with NMD (Figure 2A, compare lanes 7–8 to 3–4 and Supplementary Figure 2). Western-blot assays confirmed that UPF1 and UPF1DN proteins accumulated to comparable levels (data not shown); thus, the different effects of these proteins on NMD are not due to differences in abundance. These data strongly suggest that UPF1 plays a role in plant NMD, and that UPF1DN is a dominant-negative mutant. In further experiments, UPF1DN co-infiltration assays were used to identify NMD-targeted mRNAs.

Long 3′-UTR can act as NMD *cis* element in plant

We next wanted to identify the *cis*-acting elements of the plant NMD system. As PHA-m is a strong NMD target, whereas PHA or PHA-s mRNAs are not targeted by NMD, it is likely that sequences between the PTC of PHA-m and its original stop codon (referred to as *abc* region,
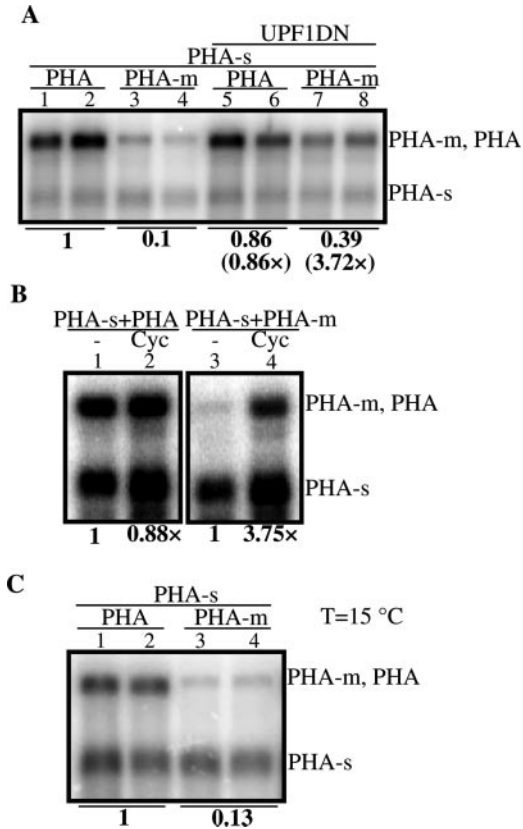
Figure 2. Agroinfiltration-based transient plant NMD assay. (**A**) Accumulation of PHA and PHA-m mRNAs in agroinfiltrated leaves. Samples were taken at 3 days post infiltration (d.p.i.) from *N.tabacum* leaves co-infiltrated with PHA + PHA-s + P14 (lanes 1 and 2), PHA-m + PHA-s + P14 (lanes 3 and 4), PHA + PHA-s + P14 + UPF1DN (lanes 5 and 6) or PHA-m + PHA-s + P14 + UPF1DN (lanes 7 and 8) cultures. Labelled PHA fragment was used as a probe. PHA and PHA-m (test) transcript levels were normalized to the levels of PHA-s internal control mRNAs. Mean values of normalized transcript levels were calculated from three independent samples (only two are shown on the blot), and then these mean transcript levels were compared. Mean value of PHA transcript levels of PHA + PHA-s + P14 infiltrated samples is taken as 1 (shown as bold number below the panel) and the test transcript levels of other samples are shown relative to it (0.1, 0,86 and 0.39, respectively). Bracketed bold numbers (shown below the relative mRNA levels) refer to the fold change, the ratio between treated and non-treated samples. PHA or PHA-m transcript levels of the UPF1DN co-infiltrated samples were compared to the corresponding PHA or PHA-m levels of PHA + PHA-s + P14 and PHA-m + PHA-s + P14 samples. Note that P14 has been co-infiltrated with each samples but P14 is not shown in the figure. (**B**) Effect of cycloheximide on the accumulation of PHA and PHA-m transcipts. PHA + PHA-s + P14 (lanes 1 and 2) and PHA-m + PHA-s + P14 (lanes 3 and 4) co-infiltrated *N.tabacum* leaves were treated with cycloheximide (Cyc) or as a control with buffer (−). PHA and PHA-m transcript levels were normalized to the PHA-s mRNA levels. The PHA and the PHA-m mRNA levels of buffer treated control samples (−) were taken as 1. The PHA and PHA-m transcript levels of Cyc treated samples are shown relative to the mRNA levels of the corresponding control samples (−). (**C**) P14 does not affect plant NMD. PHA and PHA-m agroinfiltrations, mRNA detections and quantifications were carried out as described for (A), except that P14 was not co-infiltrated. Infiltrated plants were grown at low temperature where RNA silencing is inactive.

see Figure 1) contain *cis*-acting NMD elements. To exclude the unlikely possibility that specific intramolecular interactions play a role in the instability of PHA-m transcripts, we cloned the *abc* region downstream of the stop codon of a binary GFP reporter construct (GFP-*abc*, see Figure 1). If

the *abc* region contains *cis*-acting NMD elements, GFP-*abc* mRNAs should be targeted by NMD. To test this hypothesis, *N.benthamiana* leaves were infiltrated with *Agrobacterium* carrying either the GFP-*abc* test or the GFP control construct. We found that the green fluorescence of GFP-*abc* infiltrated leaves was much weaker than the fluorescence of GFP infiltrated leaves. Moreover, GFP-*abc* mRNAs accumulated to very low levels relative to GFP mRNAs (Figure 3A). Importantly, co-infiltration of UPF1DN (Figure 3A, compare lanes 7–8 to 3–4, and see Supplementary Figure 3) or cycloheximide treatment (Figure 3B, compare lanes 3–4 to 1–2) led to selective increase of GFP-*abc* mRNA levels. These data indicate that GFP-*abc* transcripts are targeted by NMD. Thus, we concluded that the *abc* region contained all the necessary information for PTC definition.

Although it has been shown that in plants PTC-containing mRNAs transcribed from intronless genes are targeted by NMD (30–33), it is not known if DSE-like short, specific destabilizing sequences or unusually long 3′-UTRs subject these mRNAs to NMD. To distinguish between these two possibilities we tried to map the DSE-like destabilizing sequences in the *abc* region. The *abc* region was divided into three sequences ∼equal in size (∼200 nt), and then each region was cloned downstream of the stop codon of the GFP binary construct yielding GFP-*a*, GFP-*b* and GFP-*c*, respectively (Figure 1). To test if any of these constructs is targeted by NMD, GFP-*a*, GFP-*b*, GFP-*c* test and GFP control constructs were agroinfiltrated alone or were co-infiltrated with UPF1DN. We have found that GFP-*a*, GFP-*b* and GFP-*c* transcripts accumulated to comparable levels and that these mRNAs were less abundant than the control GFP transcript. It is likely that GFP-*a*, GFP-*b* and GFP-*c* mRNAs were moderately targeted by NMD because co-infiltration of UPF1DN resulted in slightly increased transcript levels (Figure 3C and Supplementary Figure 4). These data suggest that the *abc* region does not contain DSE-like destabilizing sequences, thus it is likely that the extended 3′-UTRs trigger NMD in plants. Moreover, as GFP-*abc* was much more efficiently targeted by NMD than GFP-*c* (Figure 3D), GFP-*a* or GFP-*b* (data not shown), it is likely that the length of 3′-UTR defined the efficacy of NMD. Indeed, we found that GFP-*bc* mRNAs accumulated to higher levels than GFP-*abc* but were less abundant than GFP-*b* or GFP-*c* transcripts (Figure 3D and Supplementary Figure 5).

To further confirm that long 3′-UTRs and not DSE-like sequences act as NMD *cis* elements in plants, 700, 500 and 300 nt long bacterial sequences derived from GUS gene were cloned downstream of PHA-s (P-G700, P-G500, P-G300, see Figure 1). It is unlikely that bacterial sequences contain plant DSE-like sequences, thus the finding that bacterial sequences destabilized plant transcripts further supported the model that long 3′-UTRs triggered NMD in plants (Figure 3E). Consistently, the longest GUS segment caused the strongest reduction of PHA-s mRNA levels (Figure 3E, compare lanes 7–8 to 3–4).

Introns located in the 3′-UTR could act as NMD *cis* elements in plant

Introns are efficient NMD *cis* elements in mammals. To clarify if introns located in the 3′-UTR could act as NMD
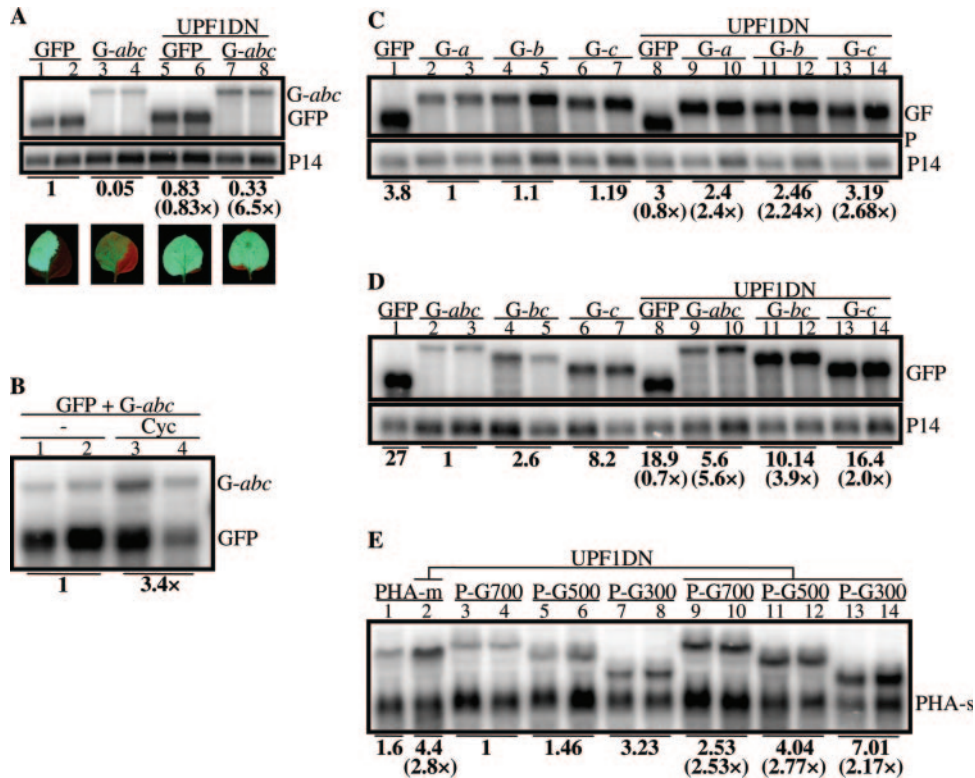
Figure 3. Long 3′-UTR acts as NMD *cis* element. (**A**) Accumulation of GFP and GFP-*abc* (shown as G-*abc*) mRNAs in leaves of *N.benthamiana* that were infiltrated with GFP + P14 (lanes 1 and 2), GFP-*abc* + P14 (lanes 3 and 4), GFP + P14 + UPF1DN (lanes 5 and 6) or GFP-*abc* + P14 + UPF1DN (lanes 7 and 8) cultures. RNA gel blot was hybridized first with a GFP probe (upper panel), then it was reprobed with P14 (lower panel). GFP and GFP-*abc* transcript levels were normalized to P14 mRNA levels. Mean GFP transcript level was taken as 1 (bold number below lower panel) and the test (GFP or GFP-*abc*) mRNA levels of other samples are shown relative to it. Bracketed numbers (lanes 5–6 and lanes 7–8) refer to the fold change of test transcript levels in the presence of UPF1DN relative to the corresponding mRNA levels obtained in the absence of UPF1DN. Photos show the GFP activity in the infiltrated leaves. (**B**) Effect of cycloheximide (Cyc) on the accumulation of GFP and GFP-*abc* (shown as G-*abc*) transcripts in *N.benthamiana* leaves. RNA gel blot was hybridized with a GFP probe. (**C**) DSE-like destabilizing sequences could not be found in the *abc* region. GFP, GFP-*a* (G-*a*), GFP-*b* (G-*b*) and GFP-*c* (G-*c*) mRNA levels were normalized to the corresponding P14 mRNA levels. Mean GFP-*a* transcript level is taken as 1. GFP, GFP-*b* and GFP-*c* transcript levels are shown relative to the level of GFP-*a*. Bracketed numbers show the fold change of corresponding test transcript levels in the presence of UPF1DN. Blot was hybridized first with the GFP probe (upper panel), then it was reprobed with P14 (lower panel). (**D**) The length of the 3′-UTR defines the efficacy of NMD. GFP-*abc* (G-*abc*), GFP-*bc* (G-*bc*), GFP-*c* (G-*c*) and GFP mRNA levels were normalized to the corresponding P14 levels, and the mean GFP-*abc* transcript level was taken as 1. (**E**) Bacterial sequences inserted into the 3′-UTR of a plant mRNA triggers NMD. The length of the inserted bacterial sequences is in correlation with the intensity of NMD. 700, 500 or 300 nt sequences from GUS gene were inserted downstream of the stop codon of PHA-s (P-G700, P-G500 and P-G300). P-G700, P-G500 and P-G300 cultures were co-infiltrated with P14 (lanes 3–8) or with P14 + UPF1DN (lanes 9–14). As a control for dominant-negative effect, PHA-m + PHA-s + P14 cultures were infiltrated or were co-infiltrated with UPF1DN (PHA-m + PHA-s + P14 + UPF1DN). These control samples were run on the same gel (lanes 1 and 2). RNA gel blot was hybridized with PHA-s probe. Samples and photos were taken at 3 d.p.i.

cis elements in plants, we cloned the well-characterized potato ST-LS1 intron (referred to as Ls) (40) downstream of the GFP-*c* reporter gene (GFP*c*-Ls, Figure 1). The effect of Ls intron on mRNA accumulation was studied in agroinfiltration assays by comparing the expression levels of the GFP*c*-Ls test and the GFP-*c* control constructs. The green fluorescence was much weaker in GFP*c*-Ls infiltrated plants than in GFP-*c* infiltrated samples (Figure 4A Supplementary Figure 6A). Consistently, GFP*c*-Ls mRNAs accumulated to low levels, while GFP-*c* mRNAs were abundant. RT–PCR assays confirmed that Ls was efficiently spliced from GFP*c*-Ls (Supplementary Figure 6C). Co-infiltration of UPF1-DN with GFP*c*-Ls resulted in stronger fluorescence and in dramatically increased GFP*c*-Ls mRNA levels (11×). Therefore, we concluded that the 3′-UTR located Ls intron could trigger NMD-mediated degradation of GFP*c*-Ls mRNA (Figure 4A and Supplementary Figure 6B). Consistent

with these data, cycloheximide treatment led to increased GFP*c*-Ls mRNA levels (Figure 4B).

To exclude that the effect of Ls intron is gene specific, we have also cloned the Ls intron 28 and 99 nt downstream of the stop codon of the PHA-s binary construct yielding P-28Ls and P-99Ls, respectively (Figure 1), and then leaves were infiltrated with either of these constructs. In these experiments PHA was used as an internal control. RT–PCR confirmed that the Ls intron was efficiently spliced from both P-28Ls and P-99Ls mRNAs (Supplementary Figure 6D). We found that P-99Ls mRNAs accumulated to low levels in the infiltrated leaves, while P-28Ls mRNAs were abundant (Figure 4C). Interestingly, co-infiltration of UPF1DN resulted in increased accumulation of P-99Ls mRNAs (4.31×) but only slightly enhanced the levels of P-28Ls mRNAs (1.66×) (Figure 4C). Consistently, cyclohex-imide treatment resulted in increased P-99Ls mRNA levels
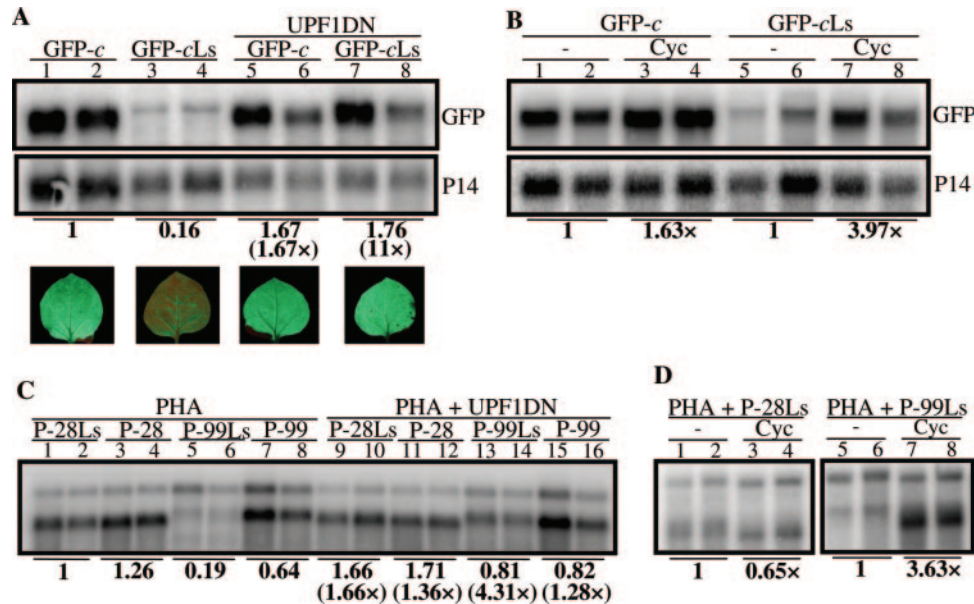
Figure 4. Introns located in the 3′-UTR could act as NMD *cis* elements. (**A**) Accumulation of the GFP-*c* and GFP-*c*Ls mRNAs in leaves of *N.benthamiana* infiltrated with GFP-*c* + P14 (lanes 1 and 2), GFP-*c*Ls+P14 (lanes 3 and 4), GFP-*c* + P14 + UPF1DN (lanes 5 and 6) or GFP-*c*Ls + P14 + UPF1DN (lanes 7 and 8) cultures. GFP-*c* and GFP-*c*Ls mRNA levels were normalized to the corresponding P14 levels, and then mean GFP-*c* mRNA level was taken as 1. Photos show the GFP activity in the infiltrated leaves. (**B**) Effect of cycloheximide (Cyc) on the accumulation of the GFP-*c* and GFP-*c*Ls transcripts. (**C**) The destabilizing effect of the 3′-UTR located Ls intron is position-dependent. *N.tabacum* leaves were infiltrated with P-28Ls + PHA + P14 or with P-99Ls + PHA + P14 + UPF1 (lanes 1–2 and 5–6, respectively). These mixtures were also co-infiltrated with UPF1DN (P-28Ls + PHA + P14 + UPF1DN, lanes 9–10, P-99Ls + PHA + P14 + UPF1DN, lanes 13–14). To exclude that the different 3′-UTR length of P-28Ls and P-99Ls transcripts is responsible for the different accumulation, identical but intronless constructs (P-28 and P-99) were infiltrated and analysed in parallel. Blot was hybridized with a PHA-s probe. Upper bands show PHA control transcripts, while the lower bands correspond to P-28Ls, P-28, P-99Ls or P-99 test mRNAs. Test mRNA levels were normalized to the corresponding PHA transcript levels. Note that the OD of the PHA control culture was 0.01, while the ODs of other cultures were 0.2. (**D**) Effect of cycloheximide (Cyc) on the accumulation of P-28Ls and P-99Ls transcripts. Samples and photos were taken at 3 d.p.i.

(3.63×) but did not lead to elevated P-28Ls mRNA levels (Figure 4D). These data suggest that introns located in the 3′-UTR can trigger NMD and that this effect is position-dependent. Plant introns located downstream but close proximity to the stop codon fail to act as NMD *cis* elements, whereas introns located more downstream of the stop codon could trigger NMD.

Tethering of UPF1 to either the 3′- or 5′-UTR of a mRNA leads to low target transcript levels

In mammals, tethering of UPF1 to the 3′-UTR of a wild-type mRNA leads to rapid degradation of the targeted mRNA (49). In contrast, tethering of UFP1 to the 5′-UTR or to the open reading frame of an intronless mRNA enhances its translation, because UPF1 promotes mRNA polysome association (50). Interestingly, UPF2, UPF3 and certain EJC proteins act similarly, tethering of these proteins to the 3′-UTR triggers rapid mRNA degradation, while their tethering to the ORF enhances translation of target mRNAs (50,51). Since introns act as NMD *cis* elements in both mammals and plants, we have postulated that in addition to NMD, plant UPF1 also stimulates translation. To test these hypotheses we constructed a binary vector, which expresses UPF1 as a λN fusion protein (λN-UPF1, Figure 1). λN specifically binds a short RNA sequence called the boxB (52,53). To create a 3′-UTR target construct, five copies of boxB as direct repeats were inserted downstream of GFP reporter gene (GFP3′boxB, see Figure 1), and then GFP3′boxB was

infiltrated alone or was co-infiltrated with λN-UPF1. As controls, GFP3′boxB was also co-infiltrated with λN or UPF1 binary constructs. While co-infiltration of λN or UPF1 affected the target mRNA levels only slightly, GFP3′boxB transcript levels were strongly reduced in λN-UPF1 co-infiltrated samples (Figure 5A, compare lanes 7–8 to 1–2 and Supplementary Figure 7). Similarly, co-infiltration of λN-UPF1 also reduced the transcript levels of P-3′boxB (see Figure 1), another 3′-UTR tethering target construct that contained five boxB repeats downstream of PHA-s reporter gene (Figure 5C). These data indicate that tethering of plant UPF1 to the 3′-UTR of a wild-type mRNA leads to downregulation of the targeted mRNA.

We next tested the effect of UPF1 tethering to the 5′-UTR of a reporter mRNA. To create a 5′-UTR tethering target construct, five boxB sequences as direct repeats were cloned into the 5′-UTR region of GFP reporter gene (GFP5′boxB, see Figure 1). GFP5′boxB was infiltrated alone or was co-infiltrated with λN-UPF1, with λN or with UPF1, respectively. Unfortunately, we failed to detect GFP activity in the GFP5′boxB infiltrated leaves (perhaps because inserted sequences contain ATGs), therefore we could not analyse the effect of 5′-UTR tethering of UPF1 on translation efficiency. However, we could study the effect of 5′-UTR tethering of UPF1 on target mRNA accumulation. Surprisingly, co-infiltration of λN-UPF1 severely reduced the levels of GFP5′boxB transcripts, while co-infiltration of λN or UPF1 did not modify the accumulation of GFP5′boxB mRNAs (Figure 5B). Tethering of UPF1 to the 5′-UTR region of
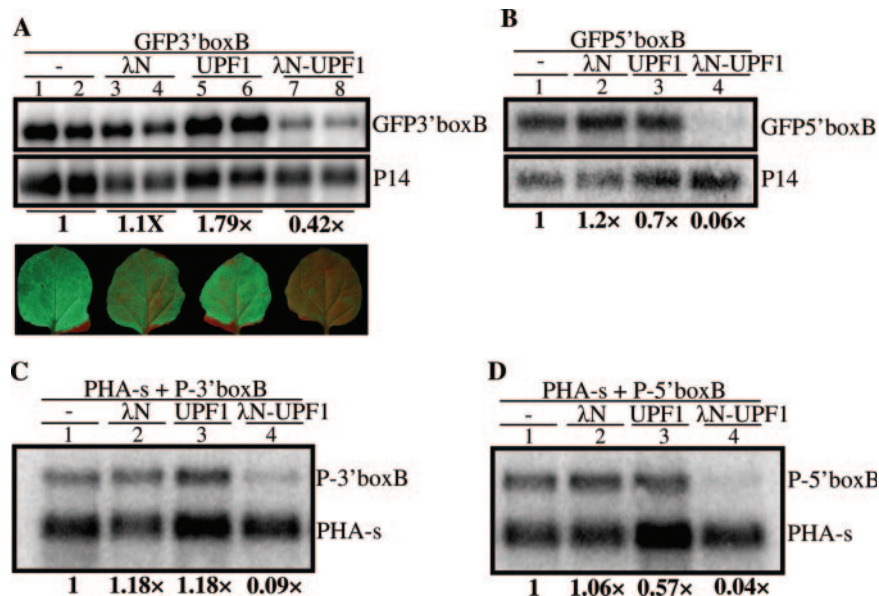
Figure 5. Tethering of UPF1 leads to reduced accumulation of target mRNAs. (**A**) Accumulation of GFP-3′boxB target mRNAs in the leaves of *N.benthamiana* co-infiltrated with GFP-3′boxB + P14 (lanes 1 and 2), GFP-3′boxB + P14 + λN (lanes 3 and 4), GFP-3′boxB + P14 + UPF1 (lanes 5 and 6) or GFP-3′boxB + P14 + λN-UPF1 (lanes 7 and 8) cultures. GFP-3′boxB mRNA levels of λN, UPF1 or λN-UPF1 co-infiltrated samples are shown relative to the GFP-3′boxB transcript level of the corresponding control (−) sample. (**B**) The effect of UPF1 tethering to the 5′-UTR of GFP-5′boxB target mRNA. (**C** and **D**) The effect of UPF1 tethering to the 3′- (P-3′boxB) or to the 5′-UTR (P-5′boxB) of the target mRNAs. PHA-s was co-infiltrated and used as an internal control. Blot was hybridized with PHA-s. Samples and photos were taken at 3 d.p.i.

the PHA-s reporter construct (P-5′boxB, see Figure 1) also led to dramatically reduced target mRNA levels (Figure 5D).

It is unlikely that tethering of UPF1 to an mRNA would lead to transcriptional silencing of the corresponding gene; therefore we suggest that tethering of UPF1 to either the 3′- or 5′-UTR causes reduced transcript accumulation because it triggers rapid degradation of targeted mRNA. As NMD is a translation-coupled decay system, the finding that 5′-UTR tethering of UPF1 also causes low transcript levels is an unexpected result. It is possible that in plants, unlike in mammals, UPF1 joins the NMD complex in a late, irreversible phase of complex formation, thus artificial tethering of UPF1 to any part of an mRNA results in rapid decay of that transcript.

DISCUSSION

Agrobacterium-based transient plant NMD assay

Transient assays have been efficiently used to analyse NMD in mammalian and *Drosophila* cells. As transient NMD assays often require the expression of several different genes, and because agroinfiltration is the best method to co-express many different genes in plants (54), we have established an agroinfiltration-based transient plant NMD test system. We have shown that PTC-containing mRNAs accumulate to low levels relative to wild-type controls and that the levels of PTC-containing mRNAs are selectively increased by cycloheximide treatment or by co-expressing UPF1DN, a dominant-negative mutant of plant UPF1 (Figures 2 and 3). These data indicate that in agroinfiltrated leaves PTC-containing mRNAs were targeted by NMD. We think that this versatile transient NMD test system, in

combination with UPF1DN co-expression and λN-boxB tethering assay systems can become useful tools to characterize plant NMD.

Cis elements of plant NMD

Taking the advantage of the transient NMD test system, we have identified the *cis* elements of plant NMD. We found that in plants stop codons are identified as PTC if the 3′-UTR is unusually long or if an intron is located in the 3′-UTR.

Previous reports have shown that intronless mRNAs can be degraded by NMD in plants (30–33). Consistently we have found that intronless mRNAs are targeted by NMD if a PTC is introduced into the coding region or if stuffer sequences are cloned into their 3′-UTRs (Figures 2 and 3). As we failed to identify DSE-like destabilizing sequences and because insertion of either bacterial or plant sequences into the 3′-UTR triggered NMD, we concluded that long 3′-UTR subjected intronless mRNAs to NMD in plants. Moreover, we have shown that this effect was size-dependent, mRNAs with longer 3′-UTR were more effectively targeted by NMD than transcript with shorter 3′-UTR (Figure 3D and E). Long 3′-UTR could also trigger NMD in yeast, *Drosophila*, worm and mammalian cells (8,17–19,55). The *faux* UTR model of yeast NMD suggests that long 3′-UTR (and perhaps other unusual 3′-UTRs) causes aberrant translation termination and that aberrant termination leads to the formation of a functional NMD complex (9). As PTC-containing yeast mRNAs can be protected from NMD if PABP is tethered downstream of the stop codon, it is likely that long 3′-UTR causes aberrant termination by inhibiting the interaction of terminating ribosome with PABP (8). Our findings that long 3′-UTR triggers NMD in

plants and that this transcript destabilizing effect depends on the size of the 3′-UTR can be explained if the *faux* UTR model is valid for plant NMD. Therefore, we suggest that aberrant translation termination also leads to NMD in plants and that increasing the distance between terminating ribosome and PABP results in aberrant termination.

Introns could also act as NMD *cis* elements in plants. The finding that incorporation of Ls intron into the 3′-UTR of either the GFP or PHA-s transcripts subjects these mRNAs to NMD (Figure 4) supports this conclusion. Moreover, the effect of plant introns on mRNA stability is position-dependent. mRNAs carrying Ls intron 99 nt downstream of the stop codon were targeted by NMD, while transcripts carrying the same intron 28 nt downstream of the stop codon did not trigger NMD (Figure 4C and D). In mammals, introns located less than 50–55 nt downstream of the stop codon also fail to trigger NMD. As 3′-UTR located introns trigger NMD in a similar position-dependent manner in both plants and mammals, we suggest that in plants, like in mammals, EJC connects splicing and NMD. Indeed, the putative orthologs of most EJC components were identified in plants (56,57). However, in plants, unlike in mammals, the 3′-UTR tethering of EJC proteins does not result in the decay of targeted mRNAs (Supplementary Figure 8). Therefore further experiments are required to prove that plant EJCs are directly involved in NMD.

Our data that introns can act as NMD *cis* elements in plants are apparently conflicting with previous studies. It has been suggested that introns do not trigger NMD in barley, because mRNAs containing introns downstream of the PTC and the control transcripts accumulated to comparable levels (35). However, the transcript which was used as a control in that study also carried a PTC, therefore the control transcript could be also targeted by NMD. Indeed, both the intron containing and control mRNAs accumulated to 3-fold lower levels than the corresponding wild-type mRNA (35). Rose has shown that incorporation of the *Arabidopsis* ubiquitin intron 80 nt downstream of the stop codon of the GUS reporter gene did not result in reduced reporter mRNA levels (36). In mammals, different introns trigger NMD with different efficiency (58). It is possible that the Ls intron triggers NMD more effectively than the ubiquitin intron. Alternatively, in plants, the intron should be more distant than 80 nt downstream of the stop codon to trigger NMD.

Identification of NMD *cis* elements allows the recognition of *Arabidopsis* genes, which could be regulated by NMD. Structural targets could be transcripts with an intron in the 3′-UTR, mRNAs with long 3′-UTR, or mRNAs containing an upstream ORF (uORF) in their 5′-UTR region. *In silico* analysis shows, that ∼30% of plant mRNAs contain uORF. We have identified ∼1000 genes whose 3′-UTRs are longer than 500 nt and found that 3.6% of all *Arabidopsis* genes contain intron in their 3′-UTRs (list of genes are available as Additional Materials, http://www.abc.hu/RNA/). Therefore, it is likely that NMD also plays a role in regulation of many wild-type genes in plants.

Evolution of PTC definition

As the putative UPF1, 2 and 3 orthologs can be identified in each eukaryotic lineages and because the NMD system has not been found in prokaryotes, it is likely that NMD evolved in the stem eukaryotes (56,59). However, the evolution of NMD system is not well understood. As long 3′-UTR triggers NMD in yeast, *Drosophila*, worm and human cells (8,17–19,55), it has been suggested that this PTC definition system is ancient (19), perhaps it was already present in the stem eukaryotes. Our result that long 3′-UTRs also trigger NMD in plants supports this hypothesis. The evolution of intron-based PTC definition is more debated. Based on the findings that introns are not NMD *cis* elements in yeast or *Drosophila*, it has been suggested that the intron-based PTC definition evolved late, only when alternative splicing had become dominant in certain animal lineages (11). An alternative model of NMD evolution has proposed that the intron-based PTC definition has already operated in the stem eukaryotes. This model suggests that splicing and NMD were coupled by the EJC in these ancient organisms (56,59). As the EJC components (56) and many introns (60,61) are highly conserved in eukaryotes, this model hypothesizes that in stem eukaryotes EJC-based NMD could efficiently eliminate PTC-containing mRNAs of spliced transcripts, thereby providing primary positive selection for the intron containing alleles. Consequently, NMD facilitated the rapid spreading of ancient introns in stem eukaryotes (56,59). The finding that 3′-UTR located introns trigger NMD in a position-dependent manner in plants is consistent with this model. This model also predicts that introns should be ∼evenly distributed within the coding regions (56,59). Indeed, we and others (59,62) have shown that plant introns are distributed relatively equally along the coding regions except the very 5′ and 3′ regions (Additional Materials).

Taken together, our findings suggest that both long 3′-UTR and intron-based PTC definition systems could operate in stem eukaryotes. In lineages, in which intron loss dominated (yeast, *Drosophila* etc.), splicing and NMD could be evolutionarily uncoupled, thus long 3′-UTR became the dominant NMD *cis* element. In contrast, in the extremely intron-dense lineages, where alternative splicing is very widely used (mammals), introns could become the more efficient and dominating NMD *cis* elements. Although, plants are intron-dense organisms, intronless genes are also frequently found in the plant genome, thus NMD machinery has evolved under dual constrains, it should efficiently identify PTC-containing mRNAs derived from either intronless or intron containing genes. Therefore, both long 3′-UTR and intron-based PTC recognition machinery should work efficiently in plants.

SUPPLEMENTARY DATA

Supplementary Data are available at NAR Online.

ACKNOWLEDGEMENTS

REFERENCES

1. Mendell,J.T., Sharifi,N.A., Meyers,J.L., Martinez-Murillo,F. and Dietz,H.C. (2004) Nonsense surveillance regulates expression of diverse classes of mammalian transcripts and mutes genomic noise. *Nature Genet.*, **36**, 1073–1078.

2. Rehwinkel,J., Letunic,I., Raes,J., Bork,P. and Izaurralde,E. (2005) Nonsense-mediated mRNA decay factors act in concert to regulate common mRNA targets. *RNA*, **11**, 1530–1544.

3. Wittmann,J., Hol,E.M. and Jack,H.M. (2006) hUPF2 silencing identifies physiologic substrates of mammalian nonsense-mediated mRNA decay. *Mol. Cell. Biol.*, **26**, 1272–1287.

4. He,F., Li,X., Spatrick,P., Casillo,R., Dong,S. and Jacobson,A. (2003) Genome-wide analysis of mRNAs regulated by the nonsense-mediated and 5′ to 3′ mRNA decay pathways in yeast. *Mol. Cell*, **12**, 1439–1452.

5. Maquat,L.E. (2004) Nonsense-mediated mRNA decay: splicing, translation and mRNP dynamics. *Nature Rev. Mol. Cell. Biol.*, **5**, 89–99.

6. Ishigaki,Y., Li,X., Serin,G. and Maquat,L.E. (2001) Evidence for a pioneer round of mRNA translation: mRNAs subject to nonsense-mediated decay in mammalian cells are bound by CBP80 and CBP20. *Cell*, **106**, 607–617.

7. Culbertson,M.R. and Neeno-Eckwall,E. (2005) Transcript selection and the recruitment of mRNA decay factors for NMD in *Saccharomyces cerevisiae*. *RNA*, **11**, 1333–1339.

8. Amrani,N., Ganesan,R., Kervestin,S., Mangus,D.A., Ghosh,S. and Jacobson,A. (2004) A faux 3′-UTR promotes aberrant termination and triggers nonsense-mediated mRNA decay. *Nature*, **432**, 112–118.

9. Amrani,N., Dong,S., He,F., Ganesan,R., Ghosh,S., Kervestin,S., Li,C., Mangus,D.A., Spatrick,P. and Jacobson,A. (2006) Aberrant termination triggers nonsense-mediated mRNA decay. *Biochem. Soc. Trans.*, **34**, 39–42.

10. Culbertson,M.R. and Leeds,P.F. (2003) Looking at mRNA decay pathways through the window of molecular evolution. *Curr. Opin. Genet. Dev.*, **13**, 207–214.

11. Tange,T.O., Nott,A. and Moore,M.J. (2004) The ever-increasing complexities of the exon junction complex. *Curr. Opin. Cell. Biol.*, **16**, 279–284.

12. Le Hir,H., Izaurralde,E., Maquat,L.E. and Moore,M.J. (2000) The spliceosome deposits multiple proteins 20–24 nucleotides upstream of mRNA exon-exon junctions. *EMBO J.*, **19**, 6860–6869.

13. Hirose,T., Shu,M.D. and Steitz,J.A. (2004) Splicing of U12-type introns deposits an exon junction complex competent to induce nonsense-mediated mRNA decay. *Proc. Natl Acad. Sci. USA*, **101**, 17976–17981.

14. Nagy,E. and Maquat,L.E. (1998) A rule for termination-codon position within intron-containing genes: when nonsense affects RNA abundance. *Trends Biochem. Sci.*, **23**, 198–199.

15. Zhang,S., Ruiz-Echevarria,M.J., Quan,Y. and Peltz,S.W. (1995) Identification and characterization of a sequence motif involved in nonsense-mediated mRNA decay. *Mol. Cell. Biol.*, **15**, 2231–2244.

16. Gonzalez,C.I., Ruiz-Echevarria,M.J., Vasudevan,S., Henry,M.F. and Peltz,S.W. (2000) The yeast hnRNP-like protein Hrp1/Nab4 marks a transcript for nonsense-mediated mRNA decay. *Mol. Cell*, **5**, 489–499.

17. Gatfield,D., Unterholzner,L., Ciccarelli,F.D., Bork,P. and Izaurralde,E. (2003) Nonsense-mediated mRNA decay in *Drosophila*: at the intersection of the yeast and mammalian pathways. *EMBO J.*, **22**, 3960–3970.

18. Pulak,R. and Anderson,P. (1993) mRNA surveillance by the *Caenorhabditis elegans* smg genes. *Genes Dev.*, **7**, 1885–1897.

19. Buhler,M., Steiner,S., Mohn,F., Paillusson,A. and Muhlemann,O. (2006) EJC-independent degradation of nonsense immunoglobulin-mu mRNA depends on 3′-UTR length. *Nature Struct. Mol. Biol.*, **13**, 462–464.

20. Amrani,N., Sachs,M.S. and Jacobson,A. (2006) Early nonsense: mRNA decay solves a translational problem. *Nature Rev. Mol. Cell. Biol.*, **7**, 415–425.

21. Conti,E. and Izaurralde,E. (2005) Nonsense-mediated mRNA decay: molecular insights and mechanistic variations across species. *Curr. Opin. Cell. Biol.*, **17**, 316–325.

22. Moore,M.J. (2005) From birth to death: the complex lives of eukaryotic mRNAs. *Science*, **309**, 1514–1518.

23. Yamashita,A., Kashima,I. and Ohno,S. (2005) The role of SMG-1 in nonsense-mediated mRNA decay. *Biochim. Biophys. Acta*, **1754**, 305–315.

24. Belostotsky,D.A. and Rose,A.B. (2005) Plant gene expression in the age of systems biology: integrating transcriptional and post-transcriptional events. *Trends Plant Sci.*, **10**, 347–353.

25. Abler,M.L. and Green,P.J. (1996) Control of mRNA stability in higher plants. *Plant Mol. Biol.*, **32**, 63–78.

26. Hori,K. and Watanabe,Y. (2005) UPF3 suppresses aberrant spliced mRNA in *Arabidopsis*. *Plant J.*, **43**, 530–540.

27. Yoine,M., Nishii,T. and Nakamura,K. (2006) *Arabidopsis* UPF1 RNA helicase for nonsense-mediated mRNA decay is involved in seed size control and is essential for growth. *Plant Cell. Physiol.*, **47**, 572–580.

28. Arciga-Reyes,L., Wootton,L., Kieffer,M. and Davies,B. (2006) UPF1 is required for nonsense-mediated mRNA decay (NMD) and RNAi in *Arabidopsis*. *Plant J.*, **47**, 480–489.

29. Yoine,M., Ohto,M.A., Onai,K., Mita,S. and Nakamura,K. (2006) The lba1 mutation of UPF1 RNA helicase involved in nonsense-mediated mRNA decay causes pleiotropic phenotypic changes and altered sugar signalling in *Arabidopsis*. *Plant J.*, **47**, 49–62.

30. Voelker,T.A., Moreno,J. and Chrispeels,M.J. (1990) Expression analysis of a pseudogene in transgenic tobacco: a frameshift mutation prevents mRNA accumulation. *Plant Cell*, **2**, 255–261.

31. van Hoof,A. and Green,P.J. (1996) Premature nonsense codons decrease the stability of phytohemagglutinin mRNA in a position-dependent manner. *Plant J.*, **10**, 415–424.

32. Dickey,L.F., Nguyen,T.T., Allen,G.C. and Thompson,W.F. (1994) Light modulation of ferredoxin mRNA abundance requires an open reading frame. *Plant Cell*, **6**, 1171–1176.

33. Petracek,M.E., Nuygen,T., Thompson,W.F. and Dickey,L.F. (2000) Premature termination codons destabilize ferredoxin-1 mRNA when ferredoxin-1 is translated. *Plant J.*, **21**, 563–569.

34. Isshiki,M., Yamamoto,Y., Satoh,H. and Shimamoto,K. (2001) Nonsense-mediated decay of mutant waxy mRNA in rice. *Plant Physiol.*, **125**, 1388–1395.

35. Gadjieva,R., Axelsson,E., Olsson,U., Vallon-Christersson,J. and Hansson,M. (2004) Nonsense-mediated mRNA decay in barley mutants allows the cloning of mutated genes by a microarray approach. *Plant Physiol. Biochem.*, **42**, 681–685.

36. Rose,A.B. (2004) The effect of intron location on intron-mediated enhancement of gene expression in *Arabidopsis*. *Plant J.*, **40**, 744–751.

37. Silhavy,D., Molnar,A., Lucioli,A., Szittya,G., Hornyik,C., Tavazza,M. and Burgyan,J. (2002) A viral protein suppresses RNA silencing and binds silencing-generated, 21- to 25-nucleotide double-stranded RNAs. *EMBO J.*, **21**, 3070–3080.

38. Merai,Z., Kerenyi,Z., Molnar,A., Barta,E., Valoczi,A., Bisztray,G., Havelda,Z., Burgyan,J. and Silhavy,D. (2005) Aureusvirus P14 is an efficient RNA silencing suppressor that binds double-stranded RNAs without size specificity. *J. Virol.*, **79**, 7217–7226.

39. Brigneti,G., Voinnet,O., Li,W.X., Ji,L.H., Ding,S.W. and Baulcombe,D.C. (1998) Viral pathogenicity determinants are suppressors of transgene silencing in *Nicotiana benthamiana*. *EMBO J.*, **17**, 6739–6746.

40. Vancanneyt,G., Schmidt,R., O'Connor-Sanchez,A., Willmitzer,L. and Rocha-Sosa,M. (1990) Construction of an intron-containing marker gene: splicing of the intron in transgenic plants and its use in monitoring early events in *Agrobacterium*-mediated plant transformation. *Mol. Gen. Genet.*, **220**, 245–250.

41. Gehring,N.H., Neu-Yilik,G., Schell,T., Hentze,M.W. and Kulozik,A.E. (2003) Y14 and hUpf3b form an NMD-activating complex. *Mol. Cell*, **11**, 939–949.

42. Voinnet,O., Lederer,C. and Baulcombe,D.C. (2000) A viral movement protein prevents spread of the gene silencing signal in *Nicotiana benthamiana*. *Cell*, **103**, 157–167.

43. Holtorf,H., Schob,H., Kunz,C., Waldvogel,R. and Meins,F., Jr (1999) Stochastic and nonstochastic post-transcriptional silencing of chitinase and beta-1,3-glucanase genes involves increased RNA turnover-possible role for ribosome-independent RNA degradation. *Plant Cell*, **11**, 471–484.

44. Szittya,G., Molnar,A., Silhavy,D., Hornyik,C. and Burgyan,J. (2002) Short defective interfering RNAs of tombusviruses are not targeted but trigger post-transcriptional gene silencing against their helper virus. *Plant Cell*, **14**, 359–372.

45. Domeier,M.E., Morse,D.P., Knight,S.W., Portereiko,M., Bass,B.L. and Mango,S.E. (2000) A link between RNA interference and nonsense-mediated decay in *Caenorhabditis elegans*. *Science*, **289**, 1928–1931.

46. Szittya,G., Silhavy,D., Molnar,A., Havelda,Z., Lovas,A., Lakatos,L., Banfalvi,Z. and Burgyan,J. (2003) Low temperature inhibits RNA silencing-mediated defence by the control of siRNA generation. *EMBO J.*, **22**, 633–640.

47. Sun,X., Perlick,H.A., Dietz,H.C. and Maquat,L.E. (1998) A mutated human homologue to yeast Upf1 protein has a dominant-negative effect on the decay of nonsense-containing mRNAs in mammalian cells. *Proc. Natl Acad. Sci. USA*, **95**, 10009–10014.

48. Leeds,P., Wood,J.M., Lee,B.S. and Culbertson,M.R. (1992) Gene products that promote mRNA turnover in *Saccharomyces cerevisiae*. *Mol. Cell. Biol.*, **12**, 2165–2177.

49. Lykke-Andersen,J., Shu,M.D. and Steitz,J.A. (2000) Human Upf proteins target an mRNA for nonsense-mediated decay when bound downstream of a termination codon. *Cell*, **103**, 1121–1131.

50. Nott,A., Le Hir,H. and Moore,M.J. (2004) Splicing enhances translation in mammalian cells: an additional function of the exon junction complex. *Genes Dev.*, **18**, 210–222.

51. Kunz,J.B., Neu-Yilik,G., Hentze,M.W., Kulozik,A.E. and Gehring,N.H. (2006) Functions of hUpf3a and hUpf3b in nonsense-mediated mRNA decay and translation. *RNA*, **6**, 1015–1027.

52. De Gregorio,E., Preiss,T. and Hentze,M.W. (1999) Translation driven by an eIF4G core domain *in vivo*. *EMBO J.*, **18**, 4865–4874.

53. Baron-Benhamou,J., Gehring,N.H., Kulozik,A.E. and Hentze,M.W. (2004) Using the lambdaN peptide to tether proteins to RNAs. *Meth. Mol. Biol.*, **257**, 135–154.

54. Voinnet,O., Rivas,S., Mestre,P. and Baulcombe,D. (2003) An enhanced transient expression system in plants based on suppression of gene silencing by the p19 protein of tomato bushy stunt virus. *Plant J.*, **33**, 949–956.

55. Mango,S.E. (2001) Stop making nonSense: the *C. elegans* smg genes. *Trends Genet.*, **17**, 646–653.

56. Lynch,M. (2006) The origins of eukaryotic gene structure. *Mol. Biol. Evol.*, **23**, 450–468.

57. Pendle,A.F., Clark,G.P., Boon,R., Lewandowska,D., Lam,Y.W., Andersen,J., Mann,M., Lamond,A.I., Brown,J.W. and Shaw,P.J. (2005) Proteomic analysis of the *Arabidopsis* nucleolus suggests novel nucleolar functions. *Mol. Biol. Cell.*, **16**, 260–269.

58. Gudikote,J.P., Imam,J.S., Garcia,R.F. and Wilkinson,M.F. (2005) RNA splicing promotes translation and RNA surveillance. *Nature Struct. Mol. Biol.*, **12**, 801–809.

59. Lynch,M. and Kewalramani,A. (2003) Messenger RNA surveillance and the evolutionary proliferation of introns. *Mol. Biol. Evol.*, **20**, 563–571.

60. Rogozin,I.B., Wolf,Y.I., Sorokin,A.V., Mirkin,B.G. and Koonin,E.V. (2003) Remarkable interkingdom conservation of intron positions and massive, lineage-specific intron loss and gain in eukaryotic evolution. *Curr. Biol.*, **13**, 1512–1517.

61. Roy,S.W. and Gilbert,W. (2005) Complex early genes. *Proc. Natl Acad. Sci. USA*, **102**, 1986–1991.

62. Sakurai,A., Fujimori,S., Kochiwa,H., Kitamura-Abe,S., Washio,T., Saito,R., Carninci,P., Hayashizaki,Y. and Tomita,M. (2002) On biased distribution of introns in various eukaryotes. *Gene*, **300**, 89–95.